

Electron Configuration and Spin Distribution in Low-Spin (*meso*-Tetraalkylporphyrinato)iron(III) Complexes Carrying One or Two Orientationally Fixed Imidazole Ligands¹

Mikio Nakamura,^{*,†,‡} Takahisa Ikeue,[‡] Hiroshi Fujii,^{*,§,⊥} Tetsuhiko Yoshimura,[§] and Kunihiko Tajima^{||}

Department of Chemistry, Toho University School of Medicine, Omorinishi, Ota-ku, Tokyo 143, Japan, Division of Biomolecular Science, Graduate School of Science, Toho University, Funabashi, Chiba 274, Japan, Institute for Life Support Technology, Yamagata Technopolis Foundation, Matsuei, Yamagata 990, Japan, and Department of Polymer Science & Technology, Kyoto Institute of Technology, Matsugasaki, Sakyo-ku, Kyoto 606, Japan

Received February 2, 1998

To understand the orientation effect of coordinated imidazole ligands, a series of low-spin (tetraalkylporphyrinato)-iron(III) complexes, $[\text{Fe}(\text{TRP})(\text{L})_2]^+$ and $[\text{Fe}(\text{TRP})(\text{L})(\text{CN})]$, carrying at least one orientationally fixed imidazole (L) have been prepared. The ¹H NMR pyrrole signals of a series of $[\text{Fe}(\text{TRP})(2\text{-MeIm})_2]^+$ have shown considerable downfield shifts as the *meso* substituent becomes bulkier, from −30.4 (R = H) to +5.6 ppm (R = ⁱPr) at −71 °C. These complexes have exhibited four pyrrole signals at lower temperature due to the hindered ligand rotation. The spread of the pyrrole signals decreases from 9.4 (Me) to 8.2 (Et) and then to 5.7 (ⁱPr) ppm. The downfield pyrrole signals together with the small spread in $[\text{Fe}(\text{T}^i\text{PrP})(2\text{-MeIm})_2]^+$ are in sharp contrast to the other low-spin complexes with orientationally fixed imidazole ligands; the chemical shifts and spreads of the pyrrole signals in [tetrakis(2,4,6-trialkylphenyl)porphyrinato]iron(III) complexes $[\text{Fe}(\text{R-TPP})(2\text{-MeIm})_2]^+$ (R = Me, Et, ⁱPr) are ca. −20 and ca. 9 ppm, respectively, at −71 °C. The EPR spectra of a series of $[\text{Fe}(\text{TRP})(2\text{-MeIm})_2]^+$ were then taken at 4.2 K. While the R = H, Me, and Et complexes have shown so-called “large g_{max} type” spectra as in the case of $[\text{Fe}(\text{R-TPP})(2\text{-MeIm})_2]^+$, the ⁱPr complex has exhibited an “axial type” spectrum. The result indicates that the electron configuration of the ferric ion of $[\text{Fe}(\text{T}^i\text{PrP})(2\text{-MeIm})_2]^+$ is presented by the unusual $(d_{xz}, d_{yz})^4(d_{xy})^1$ in contrast to the other low-spin complexes where ferric ions have the $(d_{xy})^2(d_{xz}, d_{yz})^3$ configuration. When one of the 2-MeIm ligands in $[\text{Fe}(\text{TRP})(2\text{-MeIm})_2]^+$ is replaced by CN[−], not only the ⁱPr but also the Me and Et complexes have shown the $(d_{xz}, d_{yz})^4(d_{xy})^1$ configuration as revealed from the EPR spectra. The pyrrole signals of the ⁱPr complex $[\text{Fe}(\text{T}^i\text{PrP})(2\text{-MeIm})(\text{CN})]$ have been observed at 12.2, 14.1, 14.8, and 16.2 ppm at −71 °C. Thus, the spread is only 4.0 ppm. The value is quite different from that of the corresponding $[\text{Fe}(\text{Me-TPP})(2\text{-}^i\text{PrIm})(\text{CN})]$ where the spread reaches as much as 11.4 ppm. On the basis of these results, it is concluded that the spin distribution on the pyrrole β-carbons in the complexes with $(d_{xz}, d_{yz})^4(d_{xy})^1$ is rather homogeneous even if the coordinated imidazole is orientationally fixed. On the contrary, the fixation induces a larger asymmetric spin distribution on these carbons in the complexes with $(d_{xy})^2(d_{xz}, d_{yz})^3$ configuration.

Introduction

Studies on the orientation effect of the axially coordinated imidazole ligands on the heme properties have attracted much attention in these years in connection with the biological system where the coordinated ligands are tightly fixed in the cavities of heme proteins.^{2–9} The importance of the orientation effect was originally recognized by the large spread of the heme

methyl signals in low-spin hemoproteins as compared with that of synthetic ferric porphyrin complexes with the same axial ligands.¹⁰ For example, the spread of the methyl signals in horse heart cytochrome *c*, which has histidine and methionine as axial ligands, is reported to be 30.0 ppm.¹¹ Similarly, the spreads of the methyl signals in cytochrome *b*₅ and cytochrome *c* imidazole, both of which have two imidazole ligands at the axial positions, are 20.5 and 13.5 ppm, respectively,^{12,13} as compared

* Corresponding authors. E-mail: mnakamu@med.toho-u.ac.jp.

[†] Toho University School of Medicine.

[‡] Division of Biomolecular Science, Graduate School of Science, Toho University.

[§] Institute for Life Support Technology.

[⊥] Current address: Institute for Molecular Science, Myodaiji, Okazaki 444, Japan.

^{||} Kyoto Institute of Technology.

- (1) This paper is dedicated to Professor Michinori Ōki on the occasion of his 70th birthday.
- (2) La Mar, G. N.; Walker, F. A. In *The Porphyrins*; Dolphin, D., Ed.; Academic Press: New York, 1979; Vol. IV, pp 61–157.
- (3) Bertini, I.; Luchinat, C. In *NMR of Paramagnetic Molecules in Biological Systems*; Lever, A. B. P., Gray, H. B., Eds.; Benjamin/Cummings: Menlo Park, CA, 1986; pp 165–229.

- (4) Traylor, T. G.; Berzini, A. P. *J. Am. Chem. Soc.* **1980**, *102*, 2844–2846.
- (5) Goff, H. *J. Am. Chem. Soc.* **1980**, *102*, 3252–3254.
- (6) Walker, F. A.; Buehler, J.; West, J. T.; Hinds, J. L. *J. Am. Chem. Soc.* **1983**, *105*, 6923–6929.
- (7) Scheidt, W. R.; Chipman, D. M. *J. Am. Chem. Soc.* **1986**, *108*, 1163–1167.
- (8) Walker, F. A.; Huynh, B. H.; Scheidt, W. R.; Osvath, S. R. *J. Am. Chem. Soc.* **1986**, *108*, 5288–5297.
- (9) Yamamoto, Y.; Nanai, N.; Chujo, R.; Suzuki, T. *FEBS Lett.* **1990**, *264*, 113–116.
- (10) Shulman, R. G.; Glarum, S. H.; Karplus, M. *J. Mol. Biol.* **1971**, *57*, 93–115.
- (11) Smith, M.; McLendon, G. *J. Am. Chem. Soc.* **1981**, *103*, 4912–4921.

with 3.2 ppm in protohemin bis(imidazole).² The large spreads of the methyl signals have also been observed in metmyoglobin cyanide,^{14–16} cytochrome *c* cyanide,^{11,17} lignin peroxidase cyanide,¹⁸ and HRP cyanide,¹⁸ all of which carry histidyl imidazole and cyanide as axial ligands; the spreads of the methyl signals are 22.2, 11.1, 29.3, and 25.9 ppm, respectively, as compared with 5.4 ppm in the protohemin with imidazole and cyanide.² These results suggest that naturally occurring hemoproteins have a large asymmetric spin distribution on the peripheral carbon atoms, although the degree of spread is different from protein to protein. In contrast, the synthetic complexes generally have homogeneous spin densities on the peripheral carbon atoms. The large spread of the methyl signals in hemoproteins has been reproduced even in the synthetic model complexes if they carry imidazole ligands with fixed geometry. Thus, the spread of the methyl signals in the imidazole chelated heme reaches as much as 17.1 ppm.⁴ Similarly, the pyrrole signals in the imidazole-appended heme spread over 12 ppm.^{5,6} On the basis of these studies, it is generally accepted that the fixation of the coordinated imidazole ligand induces large asymmetric spin distribution on the peripheral carbons.

Some years ago, we have reported the first example of the hindered rotation of axially coordinated imidazole ligand in bis-(2-methylimidazole){*meso*-tetrakis(2,4,6-trimethylphenyl)porphyrinato}iron(III) chloride, [Fe(Me-TPP)(2-MeIm)₂]Cl.^{19,20} Unlike the other complexes with fixed imidazole ligands, this complex is quite unique in a sense that the nonequivalence of the pyrrole protons is observed only when the rotation of the coordinated imidazole ligand is hindered. In fact, the complex showed a single pyrrole signal at a very high field, δ -10.8 ppm at 25 °C, which split into four signals, δ -14.7, -19.0, -21.0, and -23.3 ppm, at -56 °C. The spread of the pyrrole signals, 8.6 ppm at -56 °C, suggests an asymmetric spin distribution on the peripheral carbon atoms due to the fixation of the coordinated imidazole ligands. The frozen conformation in solution was determined to be the one where the ligands are placed perpendicularly along the diagonal C_{meso}-Fe-C_{meso} axes.^{21,22} The structure was further supported by the X-ray crystallographic analysis of the analogous [Fe(Me-TPP)(1,2-Me₂Im)₂]ClO₄.²³ The porphyrin ring of this complex showed a highly S₄-ruffled structure where the average deviation of the

four *meso* carbons from the mean porphyrin plane reaches as much as 0.72 Å. This indicates that the complex has two cavities developed along the diagonal C_{meso}-Fe-C_{meso} axes and that the coordinated imidazole ligands are placed in the cavities perpendicularly to each other. Thus, the solid structure is maintained even in solution.

Splitting of the pyrrole signal was commonly observed in the low-spin [tetrakis(2,4,6-trialkylphenyl)porphyrinato]iron(III) complexes [Fe(R-TPP)(L)₂]⁺ (R = Me, Et, ⁱPr) carrying a sterically hindered imidazole (L) such as 2-MeIm, 2-EtIm, 2-ⁱPrIm, 1,2-Me₂Im, 1-Me-2-ⁱPrIm, and BzIm.²⁴ The pyrrole signals of these complexes were observed at -8 to -27 ppm with the spread of 8–12 ppm at -56 °C. The EPR spectra generally showed a so-called “large g_{max} type” signal, a signal with g_{max} > 3.0 as the sole observable spectral feature.⁸ The “large g_{max} type” EPR spectra together with the extremely upfield shifted pyrrole protons in the NMR spectra clearly indicate that the ground-state electron configuration of iron is presented by the usual (d_{xy})²(d_{xz}, d_{yz})³ in which the d_{xz} and d_{yz} orbitals are nearly degenerate.^{2,25,26} The reason for the upfield shift of the pyrrole protons is ascribed to the charge transfer from the porphyrin 3e_g(x) and 3e_g(y) to the iron d_{xz} and d_{yz} orbitals, respectively, since the 3e_g orbitals have large electron densities on the pyrrole β-carbons.²⁷ Thus, the fixation of unsymmetrical 2-MeIm ligands would lower the porphyrin symmetry from D_{4h} to C₂, resulting in the asymmetric spin distribution on the porphyrin peripheral carbons. This must be one of the reasons for the spread of the four pyrrole signals, 8–12 ppm at -56 °C, in [Fe(R-TPP)(L)₂]⁺.²⁴

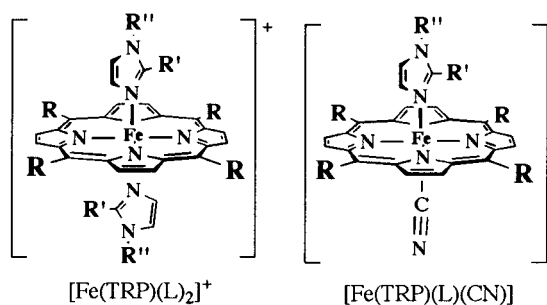
A much larger asymmetric spin distribution has been expected in the complexes with parallelly fixed imidazole ligands, since this alignment of the axial ligands can lift the degeneracy of the d_π orbitals; the unpaired electron of iron resides mainly in one of the d_π(d_{xz} and d_{yz}) orbitals which is transferred into one of the 3e_g orbitals of porphyrin, resulting in the large asymmetric spin distribution. However, there have been no reports so far on the fixation of two planar ligands in a parallel fashion on the NMR time scale. The crystallographic result mentioned above suggests that the parallel conformation must be very unstable since the second planar ligand has to coordinate to the ferric iron perpendicularly to the cavity, resulting in the large steric repulsion between the ligand and the porphyrin core. In a previous paper, we have prepared mixed-imidazole complexes such as [Fe(Et-TPP)(2-ⁱPrIm)(1-MeIm)]⁺ in which one of the axial ligands, 2-ⁱPrIm, is fixed and the other is rapidly rotating on the NMR time scale.²⁸ Since the orientation effect of the rapidly rotating ligand is canceled out, one can expect that these complexes might be good substitutes for the complex having two ligands aligned in parallel. The pyrrole signals of [Fe(Et-TPP)(2-ⁱPrIm)(1-MeIm)]⁺ appeared at δ -13.8, -18.1, -27.9, and -33.2 ppm at -56 °C. Thus, the spread of the signals increased to 19.4 ppm, which is almost twice as much as that of other complexes carrying two hindered ligands. One problem in this complex is that the 1-MeIm ligand, although rotating rapidly on the NMR time scale, still tends to take a perpendicular conformation in each moment of rotation. Thus, the better

- (12) Keller, R. M.; Wuthrich, K. *Biochim. Biophys. Acta* **1980**, *621*, 204–217.
 (13) Shao, W.; Sun, H.; Yao, Y.; Tang, W. *Inorg. Chem.* **1995**, *34*, 680–687.
 (14) Mayer, A.; Ogawa, S.; Schulman, R. G.; Yamane, T.; Cavaleiro, L. A. S.; Rocha Gonsalves, A. M. d’A.; Kenner, G. W.; Smith, K. M. *J. Mol. Biol.* **1974**, *86*, 749–756.
 (15) Emerson, S. D.; La Mar, G. N. *Biochemistry* **1990**, *29*, 1556–1566.
 (16) Banci, L.; Bertini, I.; Pierattelli, R.; Vila, A. J. *Inorg. Chem.* **1994**, *33*, 4338–4343.
 (17) Bren, K. L.; Gray, H. B.; Banci, L.; Bertini, I.; Turano, P. *J. Am. Chem. Soc.* **1995**, *117*, 8067–8073.
 (18) Banci, L.; Bertini, I.; Pierattelli, R.; Tien, M.; Vila, A. J. *J. Am. Chem. Soc.* **1995**, *117*, 8659–8667.
 (19) Nakamura, M.; Groves, J. T. *Tetrahedron* **1988**, *44*, 3225–3230.
 (20) Abbreviations: H-TPP, dianion of tetraphenylporphyrin; Me-TPP, dianion of tetrakis(2,4,6-trimethylphenyl)porphyrin or tetramesitylporphyrin; R-TPP, dianions of *meso*-tetrakis(2,4,6-trialkylphenyl)porphyrin; TRP and THP, dianions of *meso*-tetraalkylporphyrin and -porphine, respectively; Im, imidazole; 1-MeIm, 1-methylimidazole; 2-MeIm, 2-methylimidazole; 2-EtIm, 2-ethylimidazole; 2-ⁱPrIm, 2-isopropylimidazole; 1,2-Me₂Im, 1,2-dimethylimidazole; 1-Me-2-ⁱPrIm, 1-methyl-2-isopropylimidazole; BzIm, benzimidazole; 2-MeBzIm, 2-methylbenzimidazole; Py, pyridine.
 (21) Walker, F. A.; Simonis, U. *J. Am. Chem. Soc.* **1991**, *113*, 8652–8657.
 (22) Nakamura, M.; Nakamura, N. *Chem. Lett.* **1991**, 1885–1888.
 (23) Munro, O. Q.; Marques, H. M.; Debrunner, P. G.; Mohanrao, K.; Scheidt, W. R. *J. Am. Chem. Soc.* **1995**, *117*, 935–954.

- (24) Nakamura, M.; Tajima, K.; Tada, K.; Ishizu, K.; Nakamura, N. *Inorg. Chim. Acta* **1994**, *224*, 113–124.
 (25) Hatano, K.; Safo, M. K.; Walker, F. A.; Scheidt, W. R. *Inorg. Chem.* **1991**, *30*, 1643–1650.
 (26) Safo, M. K.; Gupta, G. P.; Watson, C. T.; Simonis, U.; Walker, F. A.; Scheidt, W. R. *J. Am. Chem. Soc.* **1992**, *114*, 7066–7075.
 (27) Goff, H. *Iron Porphyrins Part One*; Lever, A. B. P., Gray, H. B., Eds.; The Addison-Wesley Publishing Co.: Reading, MA, 1983; pp 237–281.
 (28) Nakamura, M. *Chem. Lett.* **1992**, 2423–2426.

candidate for the study on the orientation effect of axial ligands must be the complex carrying a planar imidazole ligand (L) and a linear cyanide ligand (CN⁻) as presented by [Fe(R-TPP)-(L)(CN)]. If rotation of the imidazole ligand is hindered, the complex would give similar information that could be obtained from the complexes with parallel fixed imidazole ligands.

Recently, we have reported another iron porphyrin system in which rotation of the coordinated 2-MeIm is hindered on the NMR time scale. They are a series of bis(2-methylimidazole)(meso-tetraalkylporphyrinato)iron(III) complexes [Fe(TRP)-(2-MeIm)₂]⁺ (R = Me, Et, and ⁱPr).²⁹ In the case of the methyl complex, the pyrrole signals started to split below -51 °C and showed four signals at δ = 6.3, -11.3, -14.4, and -15.7 ppm at -71 °C. Thus, the spread of the pyrrole signals was 9.4 ppm, which is quite close to that of [Fe(Me-TPP)(2-MeIm)₂]⁺, 8.9 ppm, at the same temperature.²⁴ In the isopropyl complex, on the contrary, the spread decreased to 3.5 ppm at -35 °C. These results suggest that the fixation of the imidazole ligand does not always induce a large asymmetric spin distribution on the peripheral carbons. Acquiring the basic knowledge of the factors which control the spin distribution on the peripheral carbons in low-spin ferric porphyrin complexes is quite important to understanding the physicochemical properties of the naturally occurring hemoproteins. Here, we report (i) the synthesis and characterization of the low-spin (meso-tetraalkylporphyrinato)iron(III) carrying orientationally fixed imidazole (L) ligands [Fe(TRP)(L)₂]⁺, (ii) the synthesis and characterization of the first examples of the mixed-ligand complexes carrying cyanide (CN) and orientationally fixed imidazole (L) ligands in both (meso-tetraalkylporphyrinato)iron(III) [Fe(TRP)-(L)(CN)] and (meso-tetramesitylporphyrinato)iron(III) [Fe(Me-TPP)(L)(CN)] complexes, (iii) the observation of the unusually small spread of the pyrrole signals in the mixed-ligand isopropyl complexes [Fe(ⁱPrP)(L)(CN)] as compared with the other complexes such as [Fe(Me-TPP)(L)₂]⁺ and [Fe(Me-TPP)(L)(CN)], and (iv) the reasons for the homogeneous spin distribution in the former complexes as compared with the latter ones.



Experimental Section

Spectral Measurement. ¹H NMR spectra were recorded on a Jeol LA300 operating at 300.4 MHz. ¹³C NMR spectra were recorded either on a Jeol LA300 operating at 75.5 MHz or on a Jeol JNM620 operating at 155.9 MHz for carbon. Chemical shifts were referenced to residual CHDCl₂ (δ = 5.32 ppm). EPR spectra were measured at 77 and 4.2 K in frozen CH₂Cl₂-CH₃OH solution with a Bruker ESP-300 spectrometer operating at X band equipped with an Oxford helium cryostat.

Synthesis. (i) [Fe(TRP)(L)₂]⁺. A series of tetraalkylporphyrins were prepared according to the literature.^{30,31} Insertion of iron was

carried out in propionic acid using FeCl₂·6H₂O. The high-spin ferric porphyrin complexes [Fe(TRP)]Cl thus obtained were purified by chromatography on silica gel using CH₂Cl₂-CH₃OH as the eluent and recrystallized from CH₂Cl₂-hexane. Bis(imidazole) complexes [Fe-(TRP)(L)₂]⁺ (R = Me, Et, ⁱPr; L = 1-MeIm, 2-MeIm, 2-ⁱPrIm) were synthesized by the addition of 2.5 mol equiv of imidazole (L) into CD₂-Cl₂ solutions of the high-spin [Fe(TRP)]Cl.²⁹

(ii) [Fe(TRP)(L)(CN)]. To a CD₂Cl₂ solution of low-spin bis(imidazole) complex [Fe(TRP)(L)₂]⁺ placed in an NMR sample tube was added KCN in CD₃OD or tetrabutylammonium cyanide (Bu₄N⁺CN⁻) in CD₂Cl₂ at -78 °C to form [Fe(TRP)(L)(CN)]. Temperature is very important to obtain the pure complex; addition of KCN at the ambient temperature resulted in the formation of both [Fe(TRP)(L)(CN)] and [Fe(TRP)(CN)₂]⁻. In the following experimental procedure to prepare the mixed-ligand complexes, only [Fe(THP)(1-MeIm)(CN)] and [Fe(TMeP)(1-MeIm)(CN)] are described in detail. All of the other complexes were prepared by the similar procedure as [Fe(TMeP)(1-MeIm)(CN)].

[Fe(THP)(1-MeIm)(CN)]. To a 300 μL CD₂Cl₂-CD₃OD (9:1) solution of [Fe(THP)]Cl (1.2 mg, 3.0 × 10⁻⁶ mol) and KCN (1.5 mol equiv) was added a CD₂Cl₂ solution of 1-MeIm at -78 °C. The reaction was monitored by ¹H NMR. The mixed-ligand complex was formed when 30 μL (3.0 mol equiv) of 1-MeIm was added as a CD₂-Cl₂ solution. Addition of a KCN solution into [Fe(THP)(1-MeIm)₂]⁺ was unsuccessful since [Fe(THP)(1-MeIm)₂]⁺ was highly insoluble in CD₂Cl₂. ¹H NMR (CD₂Cl₂-CD₃OD, -35 °C): -24.9 (8H, Py H), -0.1 (4H, meso-H), 20.0 (3H, Im-CH₃).

[Fe(TMeP)(1-MeIm)(CN)]. To a 250 μL CD₂Cl₂ solution of [Fe-(TMeP)]Cl (1.5 mg, 3.3 × 10⁻⁶ mol) placed in an NMR sample tube was added a 50 μL CD₂Cl₂ solution of 1-MeIm (3.0 mol equiv). The cooled solution (-78 °C) of the low-spin [Fe(TMeP)(1-MeIm)₂]⁺ thus formed was titrated with a CD₃OD solution of KCN. The reaction was monitored by the ¹H NMR spectrum. After the total addition of 30 μL (2.0 mol equiv to the complex) of the solution, the ¹H NMR spectrum showed a complete formation of the mixed-ligand complex [Fe(TMeP)(1-MeIm)(CN)]. ¹H NMR (CD₂Cl₂-CD₃OD, -35 °C): -6.7 (8H, Py H), 42.2 (12H, meso-CH₃), 7.5 (3H, Im-CH₃).

(iii) [Fe(Me-TPP)(L)₂]⁺. Synthesis and ¹H NMR spectra of a series of bis(imidazole) complexes of (tetramesitylporphyrinato)iron(III) [Fe-(Me-TPP)(L)₂]⁺ have already been reported in our previous paper.²⁴

(iv) [Fe(Me-TPP)(L)(CN)]. To a CD₂Cl₂ solution containing [Fe-(Me-TPP)(L)₂]⁺ was added 2.0 mol equiv of KCN at -78 °C. In the following experimental procedure to prepare the mixed-ligand complexes, only [Fe(Me-TPP)(1-MeIm)(CN)] is described in detail as a typical example. Other complexes were prepared by the similar procedure.

[Fe(Me-TPP)(1-MeIm)(CN)]. To a 250 μL CD₂Cl₂ solution of high-spin [Fe(Me-TPP)]Cl (2.1 mg, 2.4 × 10⁻⁶ mol) was added a 50 μL CD₂Cl₂ solution of 1-MeIm (3.0 mol equiv) to form the low-spin complex. To the low-spin complex thus formed was added a 30 μL of a CD₃OD solution of KCN (2.0 mol equiv) at -78 °C. Complete formation of the mixed-ligand complex was confirmed by the ¹H NMR spectral change. ¹H NMR (CD₂Cl₂-CD₃OD, 25 °C): -14.9 (8H, py H), 0.93 (12H, o-CH₃), 1.08 (12H, o-CH₃), 1.76 (12H, p-CH₃), 6.33 (4H, m-H), 6.41 (4H, m-H), 11.8 (3H, Im-CH₃).

Results

¹H NMR Spectra. (i) [Fe(TRP)(L)₂]⁺. The ¹H NMR spectra of [Fe(TRP)(1-MeIm)₂]⁺, [Fe(TRP)(2-MeIm)₂]⁺, and [Fe(TRP)(2-ⁱPrIm)₂]⁺ (R = H, Me, Et, ⁱPr) were taken in CD₂-Cl₂ at various temperatures, and their chemical shifts at -35 and -71 °C are listed in Table 1a. The pyrrole protons of the complexes having both meso-alkyl groups and bulky imidazole ligands showed signal splitting at low temperature. While the meso-unsubstituted complexes [Fe(THP)(L)₂]⁺ gave pyrrole signals at extremely high magnetic field, the ⁱPr complexes showed them in a so-called "diamagnetic region" regardless of the axial ligands. The pyrrole signals of the Me and Et complexes appeared in the middle. In general, bis(2-MeIm)

(29) Nakamura, M.; Ikeue, T.; Neya, S.; Funasaki, N.; Nakamura, N. *Inorg. Chem.* **1996**, *35*, 3731-3732.

(30) Neya, S.; Yodo, Y.; Funasaki, N. *J. Heterocycl. Chem.* **1993**, *30*, 549-550.

(31) Neya, S.; Funasaki, N. *J. Heterocycl. Chem.* **1997**, *34*, 689-690.

Table 1. ^1H NMR Chemical Shifts of a Series of Low-Spin (Tetraalkylporphyrinato)iron(III) Complexes, $[\text{Fe}(\text{TRP})(\text{L})_2]^+$,^a $[\text{Fe}(\text{TRP})(\text{CN})_2]^-$,^b and $[\text{Fe}(\text{TRP})(\text{L})(\text{CN})]^c$

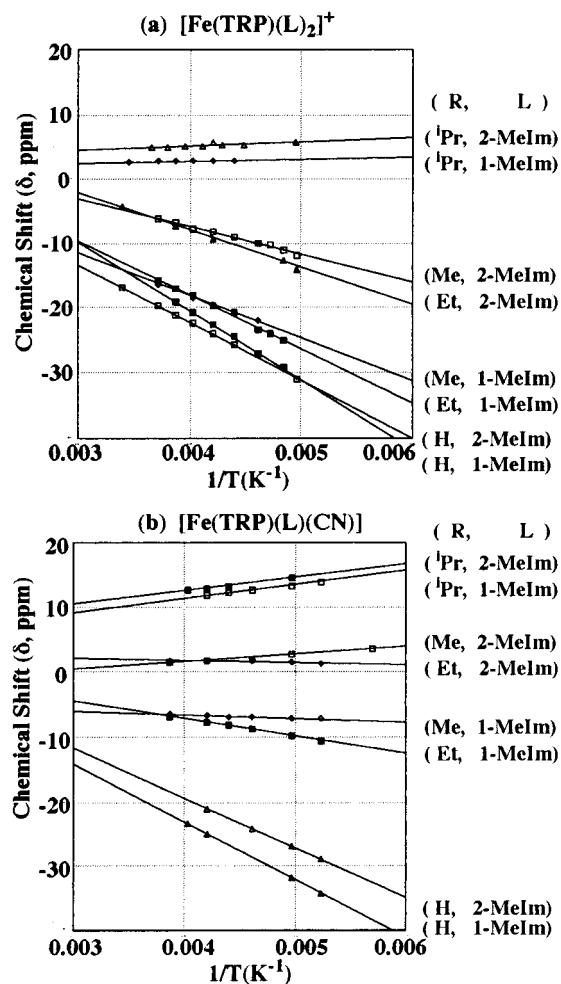
(a) $[\text{Fe}(\text{TRP})(\text{L})_2]^+$ and $[\text{Fe}(\text{TRP})(\text{CN})_2]^-$												
R	Py H of L				<i>meso</i> - α -H of L				Im-CH ₃ of L			
	1-MeIm	2-MeIm	2- ⁱ PrIm	CN ⁻	1-MeIm	2-MeIm	2- ⁱ PrIm	CN ⁻	1-MeIm	2-MeIm	2- ⁱ PrIm	
H ^c	-24.0	-22.5	<i>e</i>	-23.6					24.4	14.7	<i>e</i>	
H ^d	-30.9	-30.4	<i>e</i>	-29.2					29.9	17.5	<i>e</i>	
Me ^c	-19.6	-8.2	-7.4	0.0	8.7	38.7	39.4	64.3	19.0	3.5	-5.1	
Me ^d	-24.3	-6.3, -11.3, -14.4, -15.7	-4.9, -10.5, -12.8, -15.6	1.1	8.9	39.0, 49.6	38.8, 50.3	78.9	21.2	-1.6	-2.4, -12.4	
Et ^c	-19.7	-9.4	-7.8	-3.0	2.4	16.9	17.8	27.8	19.0	2.8	-4.8	
Et ^d	-25.9	-9.8, -14.1, -17.1, -18.0	-5.9, -10.2, -13.0, -14.3	-5.0	0.6	15.4, 16.4, 17.8	17.8, 20.5	30.3	22.9	2.2	-1.7, -10.2	
ⁱ Pr ^c	2.8	2.6, 3.8, 6.9, 7.3	2.3, 5.3, 5.3, 6.6	12.1	18.3	17.9, 21.3	15.8, 18.8	27.8	1.9	-4.5	-4.0, -9.1	
ⁱ Pr ^d	3.0	2.5, 3.9, 7.8, 8.2	2.5, 6.3, 6.7, 7.9	12.9	21.5	20.4, 25.2	17.6, 21.4	30.9	0.9	-6.8	-4.6, -10.2	

(b) $[\text{Fe}(\text{TRP})(\text{L})(\text{CN})]$												
R	Py H of L			<i>meso</i> - α -H of L			Im-CH ₃ of L					
	1-MeIm	2-MeIm	2- ⁱ PrIm	1-MeIm	2-MeIm	2- ⁱ PrIm	1-MeIm	2-MeIm	2- ⁱ PrIm			
H ^c	-24.9	-21.0	<i>e</i>	(-0.1)	(-0.2)	<i>e</i>	20.0	21.4	<i>e</i>			
H ^d	-27.1	-26.8	<i>e</i>	(-3.8)	(-2.9)	<i>e</i>	26.6	27.3	<i>e</i>			
Me ^c	-6.7	1.8	2.9	42.2	66.2	71.6	7.5	-0.8	-5.0			
Me ^d	-7.1	2.7	4.0	52.6	78.3	89.3	7.4	-2.0	-6.7			
Et ^c	-7.7	1.8	1.9	17.7	33.4	33.9	7.7	-0.3	-4.8			
Et ^d	-9.7	1.5	<i>f</i>	20.2	38.6	40.4	8.8	-0.6	-6.2			
ⁱ Pr ^c	11.7	10.8, 12.3, 12.6, 14.0	11.0, 11.8, 12.2, 14.1	25.7	27.5 (broad)	26.8 (2H), 27.2 (2H)	-2.4	-6.0	-4.8			
ⁱ Pr ^d	13.3	12.2, 14.1, 14.8, 16.2	12.2, 13.6, 14.2, 16.3	30.1	32.4 (2H), 33.1 (1H), 33.7 (1H)	32.2 (broad)	-3.6	-7.3	-5.8			

^a This work. ^b Reference 32. ^c Chemical shifts at -35°C . ^d Chemical shifts at -71°C . ^e Solubility is too low. ^f Signals are too broad.

and bis(2-ⁱPrIm) complexes exhibited the pyrrole signals at lower magnetic field than the corresponding bis(1-MeIm) complexes. In Figure 1a are given the Curie plots of the pyrrole signals in $[\text{Fe}(\text{TRP})(1\text{-MeIm})_2]^+$ and $[\text{Fe}(\text{TRP})(2\text{-MeIm})_2]^+$. Although the pyrrole protons of $[\text{Fe}(\text{TRP})(2\text{-MeIm})_2]^+$ showed four signals at low temperature, the average positions were used in the Curie plot. Except for the ⁱPr complexes, the slopes of the Curie plots were negative; both $[\text{Fe}(\text{T}^i\text{PrP})(1\text{-MeIm})_2]^+$ and $[\text{Fe}(\text{T}^i\text{PrP})(2\text{-MeIm})_2]^+$ showed small but positive slopes. For comparison, the chemical shifts of the bis(cyanide) complexes $[\text{Fe}(\text{TRP})(\text{CN})_2]^-$ are also listed in Table 1a.³²

(ii) $[\text{Fe}(\text{TRP})(\text{L})(\text{CN})]$. The ^1H NMR spectra of $[\text{Fe}(\text{TRP})(1\text{-MeIm})(\text{CN})]$, $[\text{Fe}(\text{TRP})(2\text{-MeIm})(\text{CN})]$, and $[\text{Fe}(\text{TRP})(2\text{-}^i\text{PrIm})(\text{CN})]$ were taken in $\text{CD}_2\text{Cl}_2\text{-CD}_3\text{OD}$ over a wide temperature range, -14 to -82°C . The chemical shifts at -35 and -71°C are given in Table 1b. The Curie plots of the pyrrole signals of $[\text{Fe}(\text{TRP})(1\text{-MeIm})(\text{CN})]$ and $[\text{Fe}(\text{TRP})(2\text{-MeIm})(\text{CN})]$ are given in Figure 1b. In a series of $[\text{Fe}(\text{TRP})(1\text{-MeIm})(\text{CN})]$ complexes, the unsubstituted complex (R = H) showed a pyrrole signal at $\delta -24.9$ ppm at -35°C , which is quite typical as a low-spin ferric porphyrin complex. The Me and Et complexes exhibited them at lower field, $\delta -6.7$ and -7.7 ppm at -35°C , respectively. In the case of the ⁱPr complex, the pyrrole signal appeared at fairly low field, $+11.7$ ppm. Neither pyrrole nor *meso*-alkyl signals of these complexes showed appreciable broadening even at -82°C . While the pyrrole signals of the unsubstituted and Et complexes moved to higher magnetic field as the temperature was lowered, that of the ⁱPr complex moved to the opposite direction. The pyrrole signal of the Me complex showed little dependence on temperature. The ^1H NMR signals of both the pyrrole and *meso* α -protons in $[\text{Fe}(\text{TRP})(2\text{-MeIm})(\text{CN})]$ appeared at lower magnetic field as compared with those of the corresponding $[\text{Fe}(\text{TRP})(1\text{-MeIm})(\text{CN})]$. Although the signals in the Me and Et complexes showed considerable broadening at lower temperature, they did not split even at -71°C . The clear splitting of

**Figure 1.** Curie plots of the pyrrole signals.

the signals was observed, however, in the ⁱPr complex $[\text{Fe}(\text{T}^i\text{PrP})(2\text{-MeIm})(\text{CN})]$; the pyrrole protons gave four signals with equal integral intensities at $\delta 12.2$, 14.1 , 14.8 , and 16.2 ppm and the *meso*-CH showed three signals with 2:1:1 intensity ratios

(32) Nakamura, M.; Ikeue, T.; Fujii, H.; Yoshimura, T. *J. Am. Chem. Soc.* **1997**, *119*, 6284-6291.

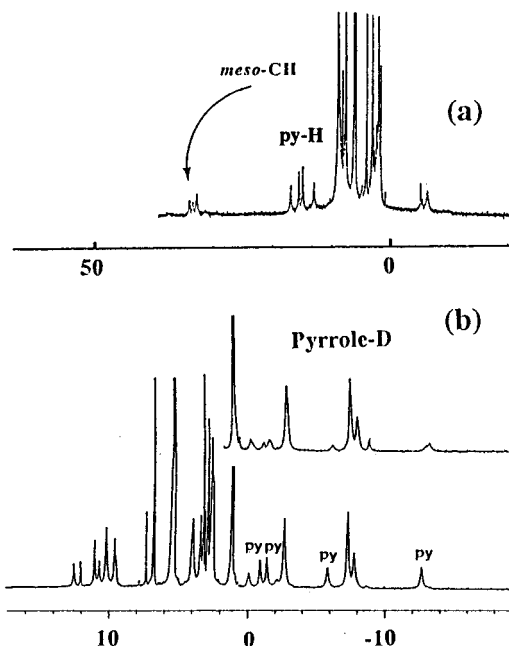


Figure 2. ^1H NMR spectra of (a) $[\text{Fe}(\text{T}'\text{PrP})(2\text{-MeIm})(\text{CN})]$ and (b) $[\text{Fe}(\text{Me-TPP})(2\text{-MeIm})(\text{CN})]$ taken at -71°C in CD_2Cl_2 . The inset shows the ^1H NMR spectrum of the corresponding pyrrole-deuterated complex taken at the same temperature.

at 32.4, 33.1, and 33.7 ppm at -71°C as shown in Figure 2a. In the case of $[\text{Fe}(\text{TRP})(2\text{-}^i\text{PrIm})(\text{CN})]$, both the pyrrole H and meso α -H signals of the isopropyl complex $[\text{Fe}(\text{T}'\text{PrP})(2\text{-}^i\text{PrIm})(\text{CN})]$ showed splitting even at -10°C ; the pyrrole protons showed four signals while the meso- α protons gave two signals with equal intensities at -35°C . The result contrasts with the case in $[\text{Fe}(\text{T}'\text{PrP})(2\text{-MeIm})(\text{CN})]$, where the meso- α protons gave three signals with 2:1:1 intensity ratio. Further lowering of the temperature caused broadening of the meso- α signals and gave a single line at -71°C .

(iii) $[\text{Fe}(\text{Me-TPP})(\text{L})_2]^+$. The ^1H NMR spectra of $[\text{Fe}(\text{Me-TPP})(\text{L})_2]^+$ have already been reported in our previous paper.²⁴ For comparison with other complexes, the chemical shifts are listed in Table 2a.

(iv) $[\text{Fe}(\text{Me-TPP})(\text{L})(\text{CN})]$. The ^1H NMR spectra of $[\text{Fe}(\text{Me-TPP})(\text{L})(\text{CN})]$ ($\text{L} = 1\text{-MeIm}, 2\text{-MeIm}, 2\text{-}^i\text{PrIm}$) were measured in $\text{CD}_2\text{Cl}_2\text{-CD}_3\text{OD}$ over a wide temperature range. The chemical shifts of these complexes at 25 and -71°C are listed in Table 2b. In $[\text{Fe}(\text{Me-TPP})(1\text{-MeIm})(\text{CN})]$, the pyrrole signal appeared at -14.9 ppm at 25°C and moved to the higher magnetic field as the temperature was lowered. The sharpness of the signal was maintained even at -71°C . In contrast, $[\text{Fe}(\text{Me-TPP})(2\text{-MeIm})(\text{CN})]$ showed a pyrrole signal at -6.3 ppm at 25°C , which broadened considerably at lower temperature and started to split below -91°C . Much clearer splitting of the signal was observed in $[\text{Fe}(\text{Me-TPP})(2\text{-}^i\text{PrIm})(\text{CN})]$, where the pyrrole signals appeared at $-12.7, -5.8, -1.4,$ and -0.9 ppm at -85°C as shown in Figure 2b. The assignment of these signals was confirmed by the spectral comparison with the corresponding pyrrole deuterated complex. The *ortho*-methyl protons also showed complicated signals at this temperature.

^{13}C NMR Spectra. The ^{13}C NMR spectra of unlabeled $[\text{Fe}(\text{TMeP})(2\text{-MeIm})_2]^+$, $[\text{Fe}(\text{TEtP})(2\text{-MeIm})_2]^+$, and $[\text{Fe}(\text{T}'\text{PrP})(2\text{-MeIm})_2]^+$ were taken at various temperatures. In these complexes, meso-carbon signals appeared at the lowest magnetic field. While the Me and Et complexes showed the meso signals at δ 195 and 200 ppm, respectively, the ^iPr complex showed two signals at much lower magnetic field, δ 323 and 394 ppm

at 25°C . When the temperature was lowered, carbon signals of the porphyrin core spread into 2 or 4 peaks even in the Me complex. Because of the low solubility and low signal-to-noise ratios, the signal assignment was not completed at low temperature. Thus, only the chemical shifts of the meso carbons at 25 and -60°C are listed in Table 3.

Spread of the Signals. The spread of the pyrrole β - and meso α -proton signals is defined by the maximum difference in chemical shifts at low temperature where the rotation of axial ligands is slowed on the NMR time scale. These values are extracted from Tables 1 and 2 and are summarized in Table 4a-c.

(i) Pyrrole Proton Signals. The spread of the pyrrole signals in $[\text{Fe}(\text{TRP})(\text{L})_2]^+$ decreased as the bulkiness of the meso substituents increased. In the case of $[\text{Fe}(\text{TRP})(2\text{-MeIm})_2]^+$, the spreads were 9.4, 8.2, and 5.7 ppm at -71°C for the Me, Et, and ^iPr complexes, respectively. Similarly, the spread decreased from 10.7 ($\text{R} = \text{Me}$) to 8.4 (Et) and then to 5.4 (^iPr) ppm in $[\text{Fe}(\text{TRP})(2\text{-}^i\text{PrIm})_2]^+$. A much smaller spread was observed in the mixed-ligand complexes $[\text{Fe}(\text{TRP})(\text{L})(\text{CN})]$, although the signal splitting was observed only in the ^iPr complexes. The spreads were 4.0 and 4.1 ppm for $[\text{Fe}(\text{T}'\text{PrP})(2\text{-MeIm})(\text{CN})]$ and $[\text{Fe}(\text{T}'\text{PrP})(2\text{-}^i\text{PrIm})(\text{CN})]$, respectively. In the case of the tetraarylporphyrin complexes, $[\text{Fe}(\text{R-TPP})(\text{L})_2]^+$, the spreads were 9.0–11.3 ppm. In contrast to the tetraalkylporphyrin system, the spread further increased when one of the axial ligands was replaced by CN^- ; the spread of $[\text{Fe}(\text{Me-TPP})(2\text{-}^i\text{PrIm})(\text{CN})]$ was 11.4 ppm as compared with 10.9 ppm in $[\text{Fe}(\text{Me-TPP})(2\text{-}^i\text{PrIm})_2]^+$.

(ii) Meso α -Proton Signals. The spread of the meso α -signals decreased on going from the bis(imidazole) complex to the corresponding mixed-ligand complex. Thus, in the 2-MeIm series, it changed from 4.8 ppm in $[\text{Fe}(\text{T}'\text{PrP})(2\text{-MeIm})_2]^+$ to 1.3 ppm in $[\text{Fe}(\text{T}'\text{PrP})(2\text{-MeIm})(\text{CN})]^+$. Similar decrease was observed in the 2- $^i\text{PrIm}$ series, from 3.8 ppm in $[\text{Fe}(\text{T}'\text{PrP})(2\text{-}^i\text{PrIm})_2]^+$ to ca. 0.4 ppm in $[\text{Fe}(\text{T}'\text{PrP})(2\text{-}^i\text{PrIm})(\text{CN})]$.

EPR Spectra. **(i) $[\text{Fe}(\text{TRP})(2\text{-MeIm})_2]^+$.** Although bis(imidazole) complexes were EPR silent at 77 K, they gave clear signals at 4.2 K as shown in Figure 3. The unsubstituted complex $[\text{Fe}(\text{THP})(2\text{-MeIm})_2]^+$, though too insoluble to obtain a spectrum with good signal-to-noise ratio, showed a large g_{max} type signal at $g = 3.45$. The Me and Et complexes exhibited broad signals at $g = 2.9$ and 3.0, respectively. In contrast, the ^iPr complex showed an axial type spectrum where a sharp signal appeared at $g = 2.58$. The EPR g values of these complexes are listed in Table 5.

(ii) $[\text{Fe}(\text{TRP})(2\text{-MeIm})(\text{CN})]$. The mixed-ligand complexes were obtained by the addition of 2.0 mol equiv of $\text{Bu}_4\text{N}^+\text{CN}^-$ as a CH_3OH solution into a CH_2Cl_2 solution of $[\text{Fe}(\text{TRP})(2\text{-MeIm})_2]^+$. The EPR spectra of these complexes taken at 4.2 K are given in Figure 4. Although the unsubstituted complex showed a large g_{max} type spectrum, the Me and Et complexes showed sharp axial type spectra. Close inspection of the figure revealed that the sample was contaminated with small amounts of bis(cyanide) and bis(imidazole) complexes. Further addition of cyanide into the solution increased the intensity of the peak ascribed to bis(cyanide). Thus, by the addition of various amounts of cyanide into $[\text{Fe}(\text{TRP})(2\text{-MeIm})_2]^+$, we were able to assign the signals derived from the mixed-ligand complex. The g values of these complexes are listed in Table 5 together with those of the corresponding $[\text{Fe}(\text{TRP})(\text{CN})_2]^-$.³²

Table 2. ^1H NMR Chemical Shifts of a Series of Low-Spin $[\text{Fe}(\text{Me-TPP})(\text{L})_2]^+$ and $[\text{Fe}(\text{Me-TPP})(\text{L})(\text{CN})]^b$

L	Py-H	<i>o</i> -Me	<i>m</i> -H	<i>p</i> -Me	Im-Me
(a) $[\text{Fe}(\text{Me-TPP})(\text{L})_2]^+$					
1-MeIm ^c	-17.2	0.8	6.0	1.7	17.0
1-MeIm ^d	-30.9	0.0	4.9	1.0	25.7
2-MeIm ^c	-10.8	1.5	7.2	2.0	5.3
2-MeIm ^d	-24.4, -22.0, -20.0, -15.4	-7.6, -3.3, 4.8, 10.8	5.5, 5.5, 6.8, 9.8	0.8, 2.2	5.0
2- ⁱ PrIm ^c	-10.8	1.8	7.6	2.9	-2.3
2- ⁱ PrIm ^d	-24.3, -21.2, -19.4, -13.4	-7.1, -2.7, 6.2, 12.5	7.2, 7.2, 7.6, 10.6	1.1, 2.7	-10.9, 0.0
(b) $[\text{Fe}(\text{Me-TPP})(\text{L})(\text{CN})]$					
1-MeIm ^c	-14.9	0.9, 1.1	6.3, 6.4	1.76	11.8
1-MeIm ^d	-23.4	0.6, 0.7	6.4, 6.5	1.46	16.3
2-MeIm ^c	-6.3	1.5, 1.7	8.1, 8.2	2.34	3.2
2-MeIm ^d	-6.1 (broad)	1.5 (broad)	9.7, 9.8	2.58	3.1
2- ⁱ PrIm ^c	-6.1	1.8, 1.9	8.20, 8.23	2.10	-2.4
2- ⁱ PrIm ^d	-12.9, -6.7, -1.9, -1.5	-6.6, -1.8, 3.5, 4.1, 5.7	8.2-10.5 ^e	2.7, 2.9	-6.2

^a Data from ref 24. ^b This work. ^c Chemical shifts at 25 °C. ^d Chemical shifts at -71 °C. ^e Several signals for the *m*-protons were observed at -85 °C at δ 9.8, 10.0, 10.5, 10.9, 11.1, and 11.5 ppm.

Table 3. ^{13}C NMR Chemical Shifts of the *Meso* Carbons in $[\text{Fe}(\text{TRP})(2\text{-MeIm})_2]\text{Cl}$ Taken in CDCl_3

R	25 °C	-60 °C	$\Delta\delta^a$
Me	194.6	148 265	117
Et	200.0	<i>b</i>	<i>b</i>
ⁱ Pr	322.5 393.8	397 507	110

^a Difference in chemical shifts at -60 °C. ^b Signals were not observed due to the low solubility.

Table 4. Spread of the Pyrrole and *Meso* α -Proton Signals at -71 °C

(a) Pyrrole Signals (Tetraalkyl Complexes) ^a				
R	$[\text{Fe}(\text{TRP})(\text{L})_2]^+$		$[\text{Fe}(\text{TRP})(\text{L})(\text{CN})]$	
	2-MeIm	2- ⁱ PrIm	2-MeIm	2- ⁱ PrIm
Me	9.4	10.7	<i>b</i>	<i>b</i>
Et	8.2	8.4	<i>b</i>	<i>b</i>
ⁱ Pr	5.7	5.4	4.0	4.1

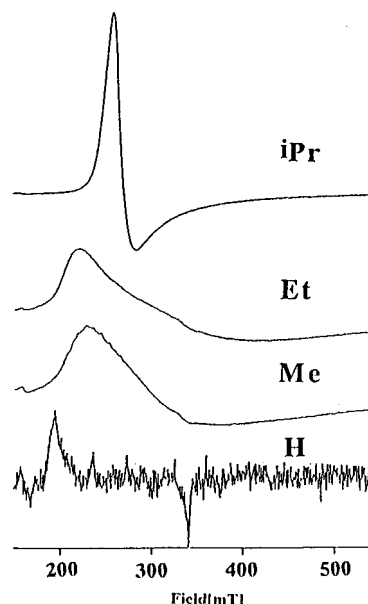
(b) Pyrrole Signals (Tetraaryl Complexes) ^c				
R	$[\text{Fe}(\text{R-TPP})(\text{L})_2]^+$		$[\text{Fe}(\text{R-TPP})(\text{L})(\text{CN})]$	
	2-MeIm	2- ⁱ PrIm	2-MeIm	2- ⁱ PrIm
Me	9.0	10.9	<i>b</i>	11.4
Et	9.5	11.3	<i>d</i>	<i>d</i>
ⁱ Pr	8.9	10.4	<i>d</i>	<i>d</i>

(c) <i>Meso</i> α -Signals (Tetraalkyl Complexes) ^a				
R	$[\text{Fe}(\text{TRP})(\text{L})_2]^+$		$[\text{Fe}(\text{TRP})(\text{L})(\text{CN})]$	
	2-MeIm	2- ⁱ PrIm	2-MeIm	2- ⁱ PrIm
Me	10.6	11.5	<i>b</i>	<i>b</i>
Et	2.4	2.7	<i>b</i>	<i>b</i>
ⁱ Pr	4.8	3.8	1.3	ca. 0.4

^a This work. ^b Signal splitting was not observed even at -71 °C. ^c Data in ref 24 were extrapolated to -71 °C. ^d Not examined.

Discussion

Stable Conformation. Low-temperature ^1H NMR spectrum of $[\text{Fe}(\text{T}^i\text{PrP})(2\text{-MeIm})(\text{CN})]$ showed four signals for the pyrrole protons and three signals for the *meso*- α protons. The intensity ratio of the latter signals was 2:1:1 as shown in Figure 2a. On the basis of the splitting pattern of the ^1H NMR signals, the frozen conformation of this complex was determined to be the one where the coordinated 2-MeIm is aligned along the $\text{C}_{\text{meso}}-\text{Fe}-\text{C}_{\text{meso}}$ axis as shown in Figure 5a. The low-temperature ^1H NMR spectra of $[\text{Fe}(\text{T}^i\text{PrP})(2\text{-}^i\text{PrIm})(\text{CN})]$ showed four signals for the pyrrole and two signals with equal intensities

**Figure 3.** EPR spectra of a series of $[\text{Fe}(\text{TRP})(2\text{-MeIm})_2]^+$ taken at 4.2 K in frozen CH_2Cl_2 solution. From the top to the bottom, R = ⁱPr, Et, Me, and H.**Table 5.** EPR Parameters of $[\text{Fe}(\text{TRP})(2\text{-MeIm})_2]^+$ (A),^a $[\text{Fe}(\text{TRP})(2\text{-MeIm})(\text{CN})]$ (B),^a and $[\text{Fe}(\text{TRP})(\text{CN})_2]^-$ (C)^b Taken at 4.2 K in $\text{CH}_2\text{Cl}_2-\text{CH}_3\text{OH}$ Solution

R	A			B			C		
	$ g_x $	$ g_y $	$ g_z $	$ g_x $	$ g_y $	$ g_z $	$ g_x $	$ g_y $	$ g_z $
H	<i>c</i>	<i>c</i>	3.45	<i>c</i>	<i>c</i>	3.3	<i>c</i>	<i>c</i>	3.5
Me	<i>c</i>	2.1	2.9	2.5	2.5	1.6 ^d	2.43	2.43	1.69
Et	<i>c</i>	1.9	3.0	2.5	2.5	1.6 ^d	2.47	2.47	1.61
ⁱ Pr	2.58	2.58	1.45 ^d	2.45	2.45	1.67	2.35	2.35	1.82

^a This work. ^b Data from ref 32. ^c Difficult to determine. ^d Calculated value.

for the *meso*- α protons. Thus, the stable conformation in this complex is consistent with the one given in Figure 5b. However, the chemical shift of one of the *meso* α -protons could coincide with the other. This is possible because the *meso* α -signals in $[\text{Fe}(\text{T}^i\text{PrP})(2\text{-MeIm})(\text{CN})]$ appeared in quite a narrow region, 32.4 (2H), 33.1 (1H), and 33.7 (1H) ppm at -71 °C. Thus, we cannot rule out the conformation given in Figure 5a. Considering the fact that the porphyrin ring in the $\text{Ni}(\text{T}^i\text{-PrP})$ is highly deformed and has two cavities along the diagonal $\text{C}_{\text{meso}}-\text{Fe}-\text{C}_{\text{meso}}$ axes,³³ it might be much reasonable to consider that the 2-ⁱPrIm ligand is placed along the cavity as in the case of $[\text{Fe}(\text{T}^i\text{PrP})(2\text{-MeIm})(\text{CN})]$.

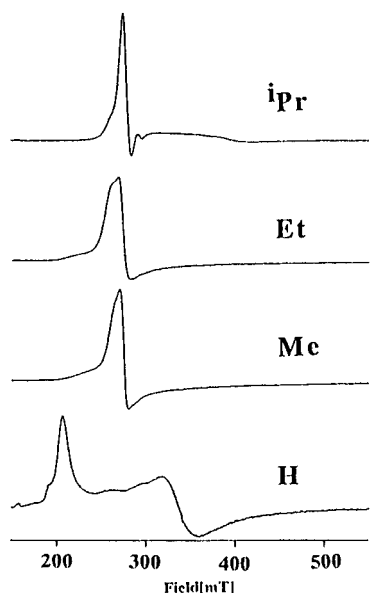


Figure 4. EPR spectra of a series of $[\text{Fe}(\text{TRP})(2\text{-MeIm})(\text{CN})]$ taken at 4.2 K in frozen $\text{CH}_2\text{Cl}_2\text{-CH}_3\text{OH}$ solution. From the top to the bottom, $\text{R} = \text{iPr}$, Et, Me, and H.

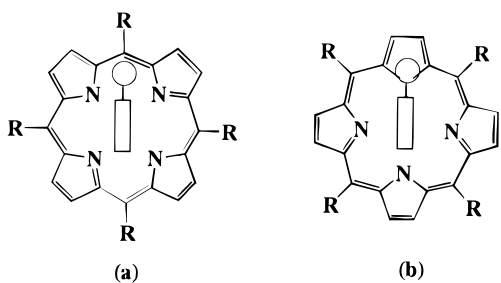


Figure 5. Conformation of the mixed-ligand complexes. The imidazole ligand is aligned along the diagonal (a) $\text{C}_{\text{meso}}\text{-Fe-C}_{\text{meso}}$ axis and (b) N-Fe-N axis.

The conformation of the coordinated imidazole ligand in $[\text{Fe}(\text{Me-TPP})(2\text{-MeIm})(\text{CN})]$ is determined to be similar to that in $[\text{Fe}(\text{T}^i\text{PrP})(2\text{-MeIm})(\text{CN})]$ on the basis of the ^1H NMR splitting pattern. Especially suggestive is the splitting pattern of the *meta* protons shown in Figure 2b. These protons showed at least five signals in the region between 9.8 and 11.5 ppm, which is only explainable by the conformation given in Figure 5a.

Electron Configuration of Iron. (i) $[\text{Fe}(\text{TRP})(\text{L})_2]^+$. The ^1H NMR data in Table 1a show that the pyrrole signal in $[\text{Fe}(\text{TRP})(\text{L})_2]^+$ moves to the lower magnetic field as the bulkiness of the *meso* substituent increases. In a series of $[\text{Fe}(\text{TRP})(2\text{-MeIm})_2]^+$ complexes, for example, the pyrrole chemical shift changed from -22.5 ppm in $[\text{Fe}(\text{THP})(2\text{-MeIm})_2]^+$ to $+5.2$ ppm (average of the four signals) in $[\text{Fe}(\text{T}^i\text{PrP})(2\text{-MeIm})_2]^+$ at -35 °C. In a previous paper, we have observed a similar phenomenon in the low-spin $[\text{Fe}(\text{TRP})(\text{CN})_2]^-$ and ascribed it to the change in electron configuration of the ferric ion from the usual $(d_{xy})^2(d_{xz}, d_{yz})^3$ in the $\text{R} = \text{H}$ complex to the unusual $(d_{xz}, d_{yz})^4(d_{xy})^1$ in the $\text{R} = \text{iPr}$ complex.³² The EPR results given in Figure 3 and Table 5 clearly indicate that the change in electron configuration also takes place in this system. In the case of $[\text{Fe}(\text{THP})(2\text{-MeIm})_2]^+$, the large g_{max} type signal centered at $g = 3.45$ was observed. This value is quite close to $g = 3.40$ of

$[\text{Fe}(\text{H-TPP})(2\text{-MeIm})_2]^+$.³⁴ Thus, the electron configuration of $[\text{Fe}(\text{THP})(2\text{-MeIm})_2]^+$ should be presented as $(d_{xy})^2(d_{xz}, d_{yz})^3$. In the case of $[\text{Fe}(\text{TMeP})(2\text{-MeIm})_2]^+$ and $[\text{Fe}(\text{TEtP})(2\text{-MeIm})_2]^+$, the EPR spectra were quite unusual in a sense that they gave single unsymmetrical signal. Although the g values of these complexes were quite small, 2.9 and 3.0 for the Me and Et complexes, respectively, their spectra resemble large g_{max} type signal in shape. Similar EPR spectra were reported by Safo et al. in bis(3-ethylpyridine)- and bis(3-chloropyridine)- $\{meso\}$ -tetramesitylporphyrinato}iron(III) complexes, which showed single-feature large g_{max} type spectra but with unusually low g values, 2.89 and 3.07, respectively.²⁶ Thus, the present EPR results together with the upfield-shifted pyrrole signals, -8.2 ($\text{R} = \text{Me}$) and -9.4 ppm ($\text{R} = \text{Et}$) at -35 °C, suggest that the ground-state electron configuration of the ferric ions in $[\text{Fe}(\text{TMeP})(2\text{-MeIm})_2]^+$ and $[\text{Fe}(\text{TEtP})(2\text{-MeIm})_2]^+$ is $(d_{xy})^2(d_{xz}, d_{yz})^3$ although the energy differences between d_{xy} and d_{xz} orbitals are expected to be much closer than that of $[\text{Fe}(\text{THP})(2\text{-MeIm})_2]^+$. In the case of $[\text{Fe}(\text{T}^i\text{PrP})(2\text{-MeIm})_2]^+$, a sharp axial type EPR signal and an extremely downfield-shifted pyrrole proton signals were observed, which clearly indicate that the electron configuration of the iron is best presented by the unusual $(d_{xz}, d_{yz})^4(d_{xy})^1$.

(ii) $[\text{Fe}(\text{TRP})(\text{L})(\text{CN})]$. The data in Table 1b show that the pyrrole protons of $[\text{Fe}(\text{TRP})(\text{L})(\text{CN})]$ appear at lower magnetic field than those of the corresponding $[\text{Fe}(\text{TRP})(\text{L})_2]^+$. In the complexes with $\text{L} = 2\text{-MeIm}$, for example, the pyrrole chemical shifts of $[\text{Fe}(\text{TRP})(2\text{-MeIm})(\text{CN})]$ were -21.0 , $+1.8$, $+1.8$, and $+12.4$ ppm at -35 °C for $\text{R} = \text{H}$, Me, Et, and iPr , respectively, as compared with -22.5 , -8.2 , -9.4 , and $+5.2$ ppm in $[\text{Fe}(\text{TRP})(2\text{-MeIm})_2]^+$. As for the unsubstituted complex, $[\text{Fe}(\text{THP})(2\text{-MeIm})(\text{CN})]$, the upfield shifted pyrrole signal together with the large g_{max} type EPR signal at $g = 3.3$ shown in Figure 4 suggests that the electron configuration should be presented by $(d_{xy})^2(d_{xz}, d_{yz})^3$. In contrast, the pyrrole signals in the Me and Et complexes appeared in a so-called *diamagnetic region*, which might be the indication that the electron configuration of these complexes changed from $(d_{xy})^2(d_{xz}, d_{yz})^3$ to $(d_{xz}, d_{yz})^4(d_{xy})^1$ by the replacement of one of the imidazole ligands with CN^- . In fact, these complexes showed axial type EPR spectra as shown in Figure 4. It is, therefore, concluded that the electron configuration of the ferric ions in $[\text{Fe}(\text{TRP})(2\text{-MeIm})(\text{CN})]$ is given by $(d_{xz}, d_{yz})^4(d_{xy})^1$ if the *meso*-carbons carry alkyl substituents.

(iii) $[\text{Fe}(\text{Me-TPP})(\text{L})_2]^+$ and $[\text{Fe}(\text{Me-TPP})(\text{L})(\text{CN})]$. As shown in Table 2a,b, all the pyrrole proton signals in $[\text{Fe}(\text{Me-TPP})(\text{L})_2]^+$ and $[\text{Fe}(\text{Me-TPP})(\text{L})(\text{CN})]$ appeared in the high-field region typical to the low-spin complexes, -30 to -6 ppm at -71 °C. Thus, the electron configuration of the ferric ions should be presented by the usual $(d_{xy})^2(d_{xz}, d_{yz})^3$, which is supported by the EPR spectra of $[\text{Fe}(\text{Me-TPP})(\text{L})_2]^+$ reported previously; $[\text{Fe}(\text{Me-TPP})(2\text{-MeIm})_2]^+$ showed a large g_{max} type spectrum with $g = 3.17$, and $[\text{Fe}(\text{Me-TPP})(\text{HIm})_2]^+$ gave rhombic spectrum with $g_z = 2.92$, $g_y = 2.29$, and $g_x = 1.57$.^{24,26} The EPR spectrum of the analogous $[\text{Fe}(\text{H-TPP})(\text{Py})(\text{CN})]$ was also reported to show a large g_{max} type signal at $g = 3.31$.³⁵

(iv) **Correlation between Pyrrole and Imidazole Methyl Shifts.** The chemical shifts of the coordinated imidazole protons can be affected by the electron configuration of the ferric ion. If the electron configuration of the ferric ion is the usual $(d_{xy})^2$ -

(33) Jentzen, W.; Simpson, M. C.; Hobbs, J. D.; Song, X.; Ema, T.; Nelson, N. Y.; Medforth, C. J.; Smith, K. M.; Veyrat, M.; Mazzanti, M.; Ramasseul, R.; Marchon, J.-C.; Takeuchi, T.; Goddard, W. A., III; Shelnutt, J. A. *J. Am. Chem. Soc.* **1995**, *117*, 11085–11097.

(34) Walker, F. A.; Reis, D.; Balke, V. L. *J. Am. Chem. Soc.* **1984**, *106*, 6888–6898.

(35) Inness, D.; Soltis, S. M.; Strouse, C. E. *J. Am. Chem. Soc.* **1988**, *110*, 5644–5650.

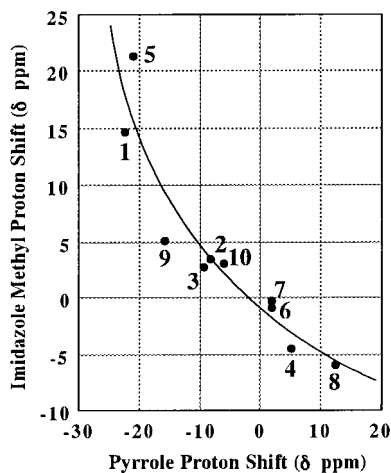


Figure 6. Correlation of the chemical shifts at $-35\text{ }^{\circ}\text{C}$ between pyrrole and imidazole methyl proton signals in a series of complexes [Fe(TRP)-(2-MeIm) $_2$] $^+$ (1, R = H; 2, R = Me; 3, R = Et; 4, R = i Pr), [Fe(TRP)-(2-MeIm)(CN)] (5, R = H; 6, R = Me; 7, R = Et; 8, R = i Pr), [Fe(Me-TPP)(2-MeIm) $_2$] $^+$ (9), and [Fe(Me-TPP)(2-MeIm)(CN)] (10).

(d_{xz} , d_{yz}) 3 , the imidazole signals are expected to appear at paramagnetically shifted positions. 36 This is because the imidazole p_{π} orbitals have correct symmetry to interact with the singly occupied iron d_{π} orbitals. In contrast, the paramagnetic shifts of the imidazole protons must be rather small in the complexes with the unusual (d_{xz} , d_{yz}) $^4(d_{xy})^1$ configuration, since the unpaired electron is in the d_{xy} orbital which is orthogonal to the imidazole p_{π} orbitals in a D_{4h} porphyrin complex. Thus, examination of the relationship between pyrrole and imidazole methyl shifts must be a good test to confirm the electron configuration of the low-spin ferric porphyrin complexes; the paramagnetic shift of the imidazole methyl protons is expected to decrease as the *meso* substituent becomes bulkier. Figure 6 shows the relationship between the pyrrole and imidazole methyl shifts in [Fe(TRP)(2-MeIm) $_2$] $^+$ and [Fe(TRP)(2-MeIm)(CN)]. As the pyrrole signals move to the lower magnetic field, in other words, as the electron configuration of the ferric ion changes from (d_{xy}) $^2(d_{xz}$, $d_{yz})^3$ to (d_{xz} , d_{yz}) $^4(d_{xy})^1$, the imidazole methyl signals shift to the higher magnetic field, from 21.4 ppm in [Fe(THP)(2-MeIm)(CN)] to -6.0 ppm in [Fe(i PrP)(2-MeIm)(CN)] at $-35\text{ }^{\circ}\text{C}$. Since the chemical shift of the imidazole methyl protons in the corresponding diamagnetic [Co(i PrP)(2-MeIm) $_2$] $^+$ is -2.3 ppm, 37 the paramagnetic shift actually decreased as the electron configuration changes from (d_{xy}) $^2(d_{xz}$, $d_{yz})^3$ to (d_{xz} , d_{yz}) $^4(d_{xy})^1$. It should be noted that the complexes 4 and 6–8 in Figure 6, all of which are located to the right and bottom of the graph, have the ferric ions with (d_{xz} , d_{yz}) $^4(d_{xy})^1$ configuration as confirmed by the EPR spectra.

Factors Stabilizing the Unusual Electron Configuration.

(i) Bulky *Meso* Substituents. In a previous paper, we have concluded that the low-spin [Fe(TRP)(CN) $_2$] $^-$ with a deformed porphyrin ring tends to have a ferric ion with the unusual electron configuration. 32 According to the recent studies on the molecular structure of a series of [Fe(TRP)Ni] complexes, the ruffling dihedral angle, defined by the $C_{\alpha}N-NC_{\alpha}$ for nitrogens in the diagonal pyrrole rings, increases as the size of the *meso* substituents increases; the angles in the Me, Et, and i Pr complexes are calculated to be 25.3, 21.0, and 36.6 $^{\circ}$, respectively. 33 The ruffling would cause two major effects on the

interaction between iron and porphyrin orbitals: (i) the decrease in the interaction between iron d_{π} (d_{xz} and d_{yz}) and porphyrin $3e_g$ orbitals due to the less effective overlap of the orbitals 32 and (ii) the increase in the interaction between iron d_{xy} and porphyrin a_{2u} orbitals as Walker and co-workers pointed out. 38,39 The weakened d_{π} and $3e_g$ interaction would stabilize the d_{π} orbitals and contribute to the formation of the unusual (d_{xz} , d_{yz}) $^4(d_{xy})^1$ electron configuration. The latter interaction, the interaction between iron d_{xy} and porphyrin a_{2u} orbitals becomes possible in the complexes with S_4 ruffled structure since the a_{2u} orbital, which is orthogonal to the d_{xy} orbital in the porphyrin complex with a D_{4h} symmetry, has xy components and thus can interact with the d_{xy} orbital. The strong $a_{2u}-d_{xy}$ interaction would destabilize the d_{xy} orbital relative to the d_{yz} and d_{xz} orbitals and contribute to the change in electron configuration from (d_{xy}) $^2(d_{xz}$, $d_{yz})^3$ to (d_{xz} , d_{yz}) $^4(d_{xy})^1$. Because of these reasons, the ferric ions in the complexes with highly S_4 -deformed porphyrin ring exhibit (d_{xz} , d_{yz}) $^4(d_{xy})^1$. Recent studies by Latos-Grazynski and co-workers using highly deformed chiorporphyrins have shown the same results. 40 One of the experimental methods to ascertain the importance of the $a_{2u}-d_{xy}$ interaction is to measure the ^{13}C NMR spectra of a series of complexes. Since the ^{13}C chemical shift directly reflects the spin densities on carbons, 41 the complexes with the (d_{xz} , d_{yz}) $^4(d_{xy})^1$ configuration are expected to show the *meso* carbon signals at more paramagnetically shifted positions than those with the (d_{xy}) $^2(d_{xz}$, $d_{yz})^3$ configuration; the a_{2u} orbital has a large spin density on the *meso* carbons. 42 The data in Table 3 indicate that, while the Me and Et complexes gave singlets at δ 194.6 and 200.0 ppm at $24\text{ }^{\circ}\text{C}$, respectively, the i Pr complex showed two signals due to the hindered rotation of the imidazole ligands at much lower magnetic field, 322.5 and 393.8 ppm. If we assume the chemical shift of the analogous diamagnetic [Co(Me-TPP)(2-MeBzIm) $_2$] $^+$, 119.5 ppm at $25\text{ }^{\circ}\text{C}$, as a diamagnetic reference, 43 the isotropic shifts of the R = Me, Et, and i Pr complexes are calculated to be 75.1, 80.5, and 238.7 ppm (average of two signals), respectively. Since the electron configuration of the Me and Et complexes is determined as (d_{xy}) $^2(d_{xz}$, $d_{yz})^3$ and that of the i Pr complex as (d_{xz} , d_{yz}) $^4(d_{xy})^1$ on the basis of the EPR results, the large spin densities on the *meso* carbons in the i Pr complex are interpreted as the consequence of the unusual electron configuration caused by the $a_{2u}-d_{xy}$ interactions in this complex. 44

(ii) Bulky Axial Ligands. The unusual electron configuration would be stabilized by the coordination of bulky imidazole ligands, since the coordination induces further deformation of the porphyrin ring. $^{23,37,45-47}$ Thus, the complexes with bulkier

(38) Safo, M. K.; Walker, F. A.; Raitsimring, A. M.; Walters, W. P.; Dolata, D. P.; Debrunner, P. G.; Scheidt, W. R. *J. Am. Chem. Soc.* **1994**, *116*, 7760–7770.

(39) Cheesman, M. R.; Walker, F. A. *J. Am. Chem. Soc.* **1996**, *118*, 7373–7380.

(40) Wolowicz, S.; Latos-Grazynski, L.; Mazzanti, M.; Marchon, J.-C. *Inorg. Chem.* **1997**, *36*, 5761–5771.

(41) Goff, H. M. *J. Am. Chem. Soc.* **1981**, *103*, 3714–3722.

(42) Fajer, J.; Davis, M. S. In *The Porphyrins*; Dolphin, D., Ed.; Academic Press: New York, 1979; Vol. IV, pp 197–256.

(43) Nakamura, M.; Ikezaki, A. *Chem. Lett.* **1995**, 733–734.

(44) A recent ^1H NMR study on the low-spin bis(cyanide) and bis(pyridine) complexes of (quinoxalino)(tetraphenylporphyrinato)iron(III) have revealed that the electron configurations of the iron(III) of these complexes are also presented as (d_{xz} , d_{yz}) $^4(d_{xy})^1$, which was explained in terms of the π -accepting nature of this porphyrin as compared with that of TPP: Wojaczynski, J.; Latos-Grazynski, L.; Glowiak, T. *Inorg. Chem.* **1997**, *36*, 6299–6306.

(45) Scheidt, W. R.; Kirner, J. F.; Hoard, J. L.; Reed, C. A. *J. Am. Chem. Soc.* **1987**, *109*, 1963–1968.

(46) Nakamura, M. *Bull. Chem. Soc. Jpn.* **1995**, *68*, 197–203.

(36) Satterlee, J. D.; La Mar, G. N. *J. Am. Chem. Soc.* **1976**, *98*, 2804–2808.

(37) Saitoh, T.; Ikeue, T.; Ohgo, Y.; Nakamura, M. *Tetrahedron* **1997**, *53*, 12487–12496.

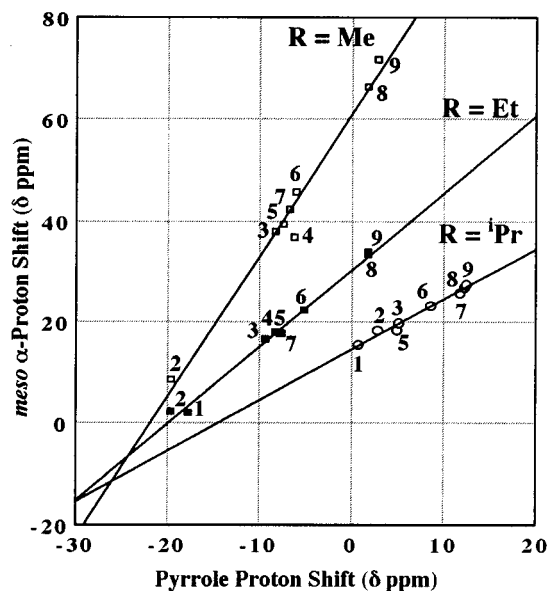


Figure 7. Correlation of the chemical shifts at -35°C between pyrrole and *meso* α -proton signals in a series of $[\text{Fe}(\text{TRP})(\text{L})_2]^+$ and $[\text{Fe}(\text{TRP})(\text{L})(\text{CN})]$ complexes. Numbers 1–6 represent the bis(imidazole) complexes $[\text{Fe}(\text{TRP})(\text{L})_2]^+$, where L is Im (1), 1-MeIm (2), 2-MeIm (3), 2-EtIm (4), 2-*i*PrIm (5), and 1,2-Me₂Im (6). Numbers 7–9 represent the mixed-ligand complexes $[\text{Fe}(\text{TRP})(\text{L})(\text{CN})]$, where L is 1-MeIm (7), 2-MeIm (8), and 2-*i*PrIm (9).

imidazole ligands are expected to show pyrrole signals at lower magnetic field than those with less bulky imidazole ligands. It is also expected that the bulky imidazole ligands shift the *meso* α -protons to further lower field due to the stronger $a_{2u}-d_{xy}$ interaction. To find out if this is the case, the correlation of the chemical shifts between the pyrrole and *meso* α -protons in $[\text{Fe}(\text{TRP})(\text{L})_2]^+$ and $[\text{Fe}(\text{TRP})(\text{L})(\text{CN})]$ was examined at -35°C . The axial ligands (L) examined are Im, 1-MeIm, 2-MeIm, 2-EtIm, 2-*i*PrIm, and 1,2-Me₂Im. The results given in Figure 7 suggest that the low-field shifts of both the pyrrole and *meso* α signals increase as the axial ligand changes in the following order: Im (1), 1-MeIm (2) < 2-MeIm (3), 2-EtIm (4), 2-*i*PrIm (5), 1-MeIm(CN⁻) (7) < 1,2-Me₂Im (6) < 2-MeIm(CN⁻) (8), 2-*i*PrIm(CN⁻) (9). Thus, the complexes with bulkier imidazole ligands generally shift both the pyrrole and *meso* α -proton signals to the lower magnetic field, supporting the hypothesis described above.

(iii) Axial Ligands with Low-Lying π^* Orbitals. Figure 7 shows that cyanide is more effective ligand than imidazole for the formation of the complexes with unusual electron configuration. This is clearly seen in the Me and Et complexes; mixed ligand complexes 1-MeIm(CN⁻) (7), 2-MeIm(CN⁻) (8), and 2-*i*PrIm(CN⁻) (9) showed pyrrole and *meso* α signals at lower magnetic field than the corresponding bis(imidazole) complexes 1-MeIm (2), 2-MeIm (3), and 2-*i*PrIm (5). It has been reported that $(d_{xz}, d_{yz})^4(d_{xy})^1$ state can be stabilized relative to $(d_{xy})^2(d_{xz}, d_{yz})^3$ by the coordination of the axial ligands with weak σ -donating and strong π -accepting ability.^{26,38,39,48–51} Although cyanide ligand is a strong σ donor, it also acts as π acceptor.

Thus, the iron d_{π} orbital can be stabilized by the cyanide π^* orbitals due to π back-bonding from metal to ligand.⁵² In the Me and Et complexes where the porphyrin deformation is shallow, d_{π} orbitals are slightly higher than the d_{xy} orbital as revealed from the EPR spectra of $[\text{Fe}(\text{TMeP})(2\text{-MeIm})_2]^+$ and $[\text{Fe}(\text{TEtP})(2\text{-MeIm})_2]^+$. Coordination of cyanide decreases the energy level of the d_{π} orbitals through $d_{\pi}-p_{\pi^*}$ interaction, resulting in the change in electron configuration from $(d_{xy})^2-(d_{xz}, d_{yz})^3$ to $(d_{xz}, d_{yz})^4(d_{xy})^1$. In the *i*Pr complexes where the porphyrin ring is highly deformed, electronic effect of the axial ligands would be less important than that in the Me and Et complexes, since the energy level of the d_{xy} orbital is already higher than that of the d_{π} orbitals. This is the reason why the chemical shifts of the pyrrole and *meso* α -protons in the *i*Pr complexes are less dependent on the axial ligands than those of the Me and Et complexes; pyrrole signals in the *i*Pr complexes appeared in a relatively narrow region, δ 0.2–12.3 ppm, as compared with those of the Me complexes, δ -19.6 to 2.9 ppm.

Common NMR Features of the Complexes with $(d_{xz}, d_{yz})^4-(d_{xy})^1$ Configuration. Figure 7 clearly shows that the complexes with $(d_{xz}, d_{yz})^4(d_{xy})^1$ configuration have pyrrole signals at much lower field than those with $(d_{xy})^2(d_{xz}, d_{yz})^3$. The borderline of the chemical shifts separating the two classes of complexes seems to be around 0 ppm at -35°C in the complexes examined in this study. In the Me and Et series, the complexes 8 and 9 satisfy this condition. The electron configuration of 8 has already been confirmed to be $(d_{xz}, d_{yz})^4-(d_{xy})^1$ by the EPR spectra. Although the EPR spectrum of 9 is not available, the ferric ion of this complex is supposed to have the $(d_{xz}, d_{yz})^4(d_{xy})^1$ configuration on the basis of the NMR chemical shifts. In the case of the *i*Pr series, all the complexes examined satisfy the condition, indicating that the electron configuration of these complexes should be presented by $(d_{xz}, d_{yz})^4(d_{xy})^1$ regardless of the axial ligands.

Another common feature of the complexes with the unusual electron configuration appears in the slopes of the Curie plots. The Curie plots of the pyrrole signals in the low-spin ferric porphyrin complexes usually give large negative slopes ranging from -9000 to -5000 ppm·K in the case of $[\text{Fe}(\text{R-TPP})(\text{L})_2]^+$.^{24,53} In fact, the Curie slopes of the typical low-spin complexes examined in this study such as $[\text{Fe}(\text{THP})(1\text{-MeIm})_2]^+$ and $[\text{Fe}(\text{THP})(2\text{-MeIm})(\text{CN})]$ were -8900 and -7700 ppm·K, respectively, as shown in Figure 1a,b. As the *meso* substituent and imidazole ligand become bulkier, the Curie slope gradually increased; the slopes in $[\text{Fe}(\text{TEtP})(2\text{-MeIm})_2]^+$ and $[\text{Fe}(\text{TEtP})(1\text{-MeIm})(\text{CN})]$ were -5800 and -2700 ppm·K, respectively. All of these complexes are supposed to have the ferric ions with the usual $(d_{xy})^2(d_{xz}, d_{yz})^3$ electron configuration as judged from their pyrrole shifts and/or EPR spectra. On the contrary, the Curie slopes were positive in the complexes with $(d_{xz}, d_{yz})^4-(d_{xy})^1$ configuration; the slopes of $[\text{Fe}(\text{T}^i\text{PrP})(2\text{-MeIm})_2]^+$, $[\text{Fe}(\text{TMeP})(2\text{-MeIm})(\text{CN})]$, and $[\text{Fe}(\text{T}^i\text{PrP})(2\text{-MeIm})(\text{CN})]$ were +660, +1100 and +2000 ppm·K, respectively. The only exception was $[\text{Fe}(\text{TEtP})(2\text{-MeIm})(\text{CN})]$, which showed a very small negative slope, -370 ppm·K. Thus, the ¹H NMR spectral features of $[\text{Fe}(\text{TRP})(\text{L})_2]^+$ and $[\text{Fe}(\text{TRP})(\text{L})(\text{CN})]$, where the ferric ions are presented by $(d_{xz}, d_{yz})^4(d_{xy})^1$, include a *downfield shift* (lower than 0 ppm) and a *positive Curie slope* of the pyrrole

(47) Momot, K. I.; Walker, F. A. *J. Phys. Chem. A* **1997**, *101*, 2787–2795.

(48) Simonneaux, G.; Hindre, F.; Le Plouzennec, M. *Inorg. Chem.* **1989**, *28*, 823–825.

(49) Guillemot, M.; Simonneaux, G. *J. Chem. Soc., Chem. Commun.* **1995**, 2093–2094.

(50) Walker, F. A.; Nasri, H.; Turowska-Tyrk, I.; Mohanrao, K.; Watson, C. T.; Shokhirev, N. V.; Debrunner, P. G.; Scheidt, W. R. *J. Am. Chem. Soc.* **1996**, *118*, 12109–12118.

(51) Pilard, M.-A.; Guillemot, M.; Toupet, L.; Jordanov, J.; Simonneaux, G. *Inorg. Chem.* **1997**, *36*, 6307–6314.

(52) Lukas, B.; Silver, J. *Inorg. Chim. Acta* **1986**, *124*, 97–100.

(53) Walker, F. A.; Simonis, U.; Zhang, H.; Walker, J. M.; Ruscitti, T. M.; Kipp, C.; Amputch, M. A.; Castillo, B. V., III; Cody, S. H.; Wilson, D. L.; Graul, R. E.; Yong, G. J.; Tobin, K.; West, J. T.; Barichievich, B. A. *New J. Chem.* **1992**, *16*, 609–620.

signals. The complexes that satisfy these ^1H NMR spectral features are considered to exhibit axial type EPR spectra.

Spin Distribution on the Peripheral Carbons. The data in Table 4 indicate that the spread of the pyrrole proton signals decreases as the *meso* substituent becomes bulkier. In the case of $[\text{Fe}(\text{TRP})(2\text{-MeIm})_2]^+$, the spread was 9.4 (Me), 8.2 (Et) and 5.7 (^iPr) ppm at -71°C . In the mixed-ligand complexes such as $[\text{Fe}(\text{T}^i\text{PrP})(2\text{-MeIm})(\text{CN})]$ and $[\text{Fe}(\text{T}^i\text{PrP})(2\text{-}^i\text{PrIm})(\text{CN})]$, the spread further decreased to 4.0 and 4.1 ppm, respectively, indicating that the spin densities on the pyrrole β -carbons are quite homogeneous. In contrast, the spread of the pyrrole signals in tetramesitylporphyrin system was much larger; it was 9.0 ppm in $[\text{Fe}(\text{Me-TPP})(2\text{-MeIm})_2]^+$, 10.9 ppm in $[\text{Fe}(\text{Me-TPP})(2\text{-}^i\text{PrIm})_2]^+$, and 11.4 ppm in $[\text{Fe}(\text{Me-TPP})(2\text{-}^i\text{PrIm})(\text{CN})]$ at -71°C . Since the complexes with relatively small spread of the pyrrole signals such as $[\text{Fe}(\text{T}^i\text{PrP})(2\text{-MeIm})_2]^+$ and $[\text{Fe}(\text{T}^i\text{PrP})(2\text{-MeIm})(\text{CN})]$ showed axial type EPR spectra, it might be natural to consider that the homogeneous spin densities on the pyrrole β -carbons are the consequence of the unusual $(d_{xz}, d_{yz})^4(d_{xy})^1$ configuration.

The similar trend was observed in the relationship between the spread of *meso* α -proton signals and the EPR g values, though the data for the comparison are quite limited. The spreads of *meso*-CH signals and EPR g_{\perp} values in $[\text{Fe}(\text{T}^i\text{PrP})(2\text{-MeIm})(\text{CN})]$ were 1.3 ppm (-71°C) and 2.45 (4.2 K), respectively, while those in $[\text{Fe}(\text{T}^i\text{PrP})(2\text{-MeIm})_2]^+$ were 4.8 ppm and 2.58. Since the g_{\perp} value of the former is smaller than that of the latter, the ferric ion in the former must have a much purer $(d_{xz}, d_{yz})^4(d_{xy})^1$ configuration.^{26,54–56} In fact, the energy differences between d_{xy} and $d\pi$ orbitals calculated based on the EPR g values were 3.48λ and 2.14λ for $[\text{Fe}(\text{T}^i\text{PrP})(2\text{-MeIm})(\text{CN})]$ and $[\text{Fe}(\text{T}^i\text{PrP})(2\text{-MeIm})_2]^+$, respectively. This means that the ferric ion of the former has 94% $(d_{xz}, d_{yz})^4(d_{xy})^1$ character while that of the latter has 84%. It is noteworthy that the *meso*-CH signals in $[\text{Fe}(\text{T}^i\text{PrP})(2\text{-MeIm})(\text{CN})]$ appeared at rather low field, 32.4, 33.1, and 33.7 ppm, as compared with those in $[\text{Fe}(\text{T}^i\text{PrP})(2\text{-MeIm})_2]^+$, 20.4 and 25.2 ppm. The results indicate

that the spin densities on the *meso* carbons in $[\text{Fe}(\text{T}^i\text{PrP})(2\text{-MeIm})(\text{CN})]$ are much more homogeneous than those in $[\text{Fe}(\text{T}^i\text{PrP})(2\text{-MeIm})_2]^+$, although the spin densities themselves are larger in the former than in the latter.

Direct evidence for the spin distribution on the *meso* carbons was obtained from the ^{13}C NMR chemical shift. While the *meso* carbon signals of the Me complex was observed at 148 and 265 ppm at -60°C , those of the ^iPr complex appeared at much lower field, 397 and 507 ppm at the same temperature. These data indicate that the spin densities of the *meso* carbons in the ^iPr complex with $(d_{xz}, d_{yz})^4(d_{xy})^1$ configuration are much larger than those in the Me complex with $(d_{xy})^2(d_{xz}, d_{yz})^3$ configuration, although the difference in spin densities among four *meso* carbons is quite similar between these two complexes; the chemical shift differences at -60°C were 117 and 110 ppm, respectively. The results suggest that the spin densities among four *meso* carbons are much more homogeneous in the ^iPr complex than in the Me complex.

Conclusion

Combined ^1H and ^{13}C NMR and EPR studies of a series of low-spin ferric porphyrin complexes, $[\text{Fe}(\text{TRP})(\text{L})_2]^+$ and $[\text{Fe}(\text{TRP})(\text{L})(\text{CN})]$, where R = H, Me, Et, or ^iPr and L is 1-MeIm, 2-MeIm, or 2- $^i\text{PrIm}$, have revealed that electron configuration of these complexes changes from $(d_{xy})^2(d_{xz}, d_{yz})^3$ to $(d_{xz}, d_{yz})^4(d_{xy})^1$ as the bulkiness of *meso*-alkyl group increases. When the rotation of axially coordinated 2-MeIm or 2- $^i\text{PrIm}$ is frozen at low temperature on the NMR time scale, both the pyrrole β - and *meso* α -proton signals as well as the *meso*-carbon signals have shown splitting. On the basis of the chemical shifts and the spreads of these signals, it is concluded that the major spin densities in the complexes with $(d_{xz}, d_{yz})^4(d_{xy})^1$ electron configuration are on the *meso*-carbons and that the spin distributions on the four *meso* carbons as well as on the eight pyrrole β -carbons are quite homogeneous. On the contrary, the major spin densities in the complexes with $(d_{xy})^2(d_{xz}, d_{yz})^3$ electron configuration are on the pyrrole β -carbons and the fixation of the coordinated imidazole ligands induces relatively large asymmetric spin distribution both on the four *meso*- and on the eight pyrrole β -carbons.

IC9801241

(54) Taylor, C. P. S. *Biochim. Biophys. Acta* **1977**, *491*, 137–149.

(55) Bohan, T. L. *J. Magn. Reson.* **1977**, *26*, 109–118.

(56) Palmer, G. In *Iron Porphyrins Part Two*; Lever, A. B. P., Gray, H. B., Eds.; Addison-Wesley Publishing Co.: Reading, MA, 1983; pp 43–88.